

## Characterization of Metal/Cobalt Ferrite Magnetic Thin Films

C. H. Park, J. G. Na, \*N. H. Heo, \*\*S. R. Lee, \*\*\*J. Kim and \*\*\*\*K. Park

*Korea Institute of Science and Technology, P. O. Box 131, Cheongyang, Seoul 130-650, Korea. \*Materials and Corrosion Lab., KEPRI, Taejeon, 305-380, Korea. \*\*Department of Metals Engineering, Korea University, Seoul 136-701, Korea. \*\*\*Department of Metals Engineering, Hanyang University, Ansan 425-791, Korea. \*\*\*\*Department of Materials Engineering, Chung-ju National University, Chungbuk 380-702, Korea.*

(Received 24 September 1997)

Metal/cobalt ferrite composite thin films with the saturation magnetization ( $M_s$ ) of  $\sim 580$  emu/cm<sup>3</sup> and the coercivity ( $H_c$ ) of 1700 Oe were prepared by the reactive sputtering. With increasing substrate temperature,  $M_s$  of the thin films increased, while  $H_c$  of the thin films decreased. This is attributed to the precipitation of  $\text{Co}_x\text{Fe}_{1-x}$  ( $x \approx 0.62$ ) metal phase in the thin films. The metal phase showed the BCC structure ( $a_0 = 2.89$  Å) and  $\text{Im}\bar{3}m$  space group. Also, the cobalt ferrite phase was identified as  $\text{CoFe}_2\text{O}_4$  with a cubic structure ( $a_0 = 8.39$  Å) and a space group of  $\text{Fd}\bar{3}m$ . For the higher cobalt content than the stoichiometric composition,  $\text{Co}_{37.8}\text{Fe}_{62.2}$ , the thin films with high  $M_s$  and  $H_c$  could be obtained in the wide substrate temperature range (200-400 °C).

### 1. Introduction

Cobalt ferrite thin films are very promising materials for the magnetic recording media and thin film device applications because of high crystalline anisotropy energy, good chemical stability, and mechanical wear resistance [1, 2]. The excellent magnetic properties of the cobalt ferrite are known to be mainly attributed to the Co ions in a spinel lattice.

Cobalt ferrite has an inverse spinel structure, with half of the  $\text{Fe}^{3+}$  ions on tetrahedral sites (A sites) and the rest, together with  $\text{Co}^{2+}$  ions, on octahedral sites (B sites) at room temperature. According to the one-ion crystalline-field model, the strong anisotropy of  $\text{Co}^{2+}$  ion on the B site originates from incompletely quenched angular momentum, which is attributed to the interaction of the electronic structure of  $\text{Co}^{2+}$  ions with the crystal field [3].

The thin films have some problems to be solved before their application can be realized. One of the problems is the low saturation magnetization ( $M_s$ ) of the thin films, less than half of that of the metallic thin films. In this study, metal/cobalt ferrite composite thin films were prepared by a reactive sputtering.

The microstructure of the thin films was investigated by X-ray diffraction (XRD) and transmission electron microscopy (TEM). TEM studies were done by primitive cell volume measurement and convergent beam electron diffraction (CBED) pattern analysis, which can be a simple and reliable method for

the identification of the metal and ferrite phases [4-7]. The valency state of the Co and Fe elements and the cation distribution in the spinel lattice were analyzed by X-ray photoelectron spectroscopy (XPS).

### 2. Experimental Procedure

Metal/cobalt ferrite composite thin films were prepared by controlling the sputtering conditions, such as oxygen concentration in sputtering gas, substrate temperature, and composition of the thin films using a facing targets-sputtering unit. Three  $\text{Co}_x\text{Fe}_{1-x}$  alloys ( $x = 28.5, 33.7, \text{ and } 37.8$  at.%) were deposited, i.e., hypostoichiometric, stoichiometric, and hyperstoichiometric compositions of cobalt ferrite. The sputter gas was a mixture of Ar (99.999 at.% purity) and  $\text{O}_2$  (99.99 at.% purity) and each gas was introduced into the chamber independently. Targets were composed of 60-mm-diameter iron discs (99.9 at.% purity) and cobalt chips (99.9 at.% purity). The cobalt content of ferrite thin films was controlled by adjusting the number of cobalt chips attached on the iron discs. Prior to deposition, the targets were presputtered at  $1.0 \times 10^{-3}$  Torr for 30 min to remove impurities on the targets. Thermally oxidized Si wafers were used as substrates. Detailed sputtering conditions are summarized in Table 1.

The cross-sectional and plan-view TEM specimens were mechanically ground to  $\sim 120$   $\mu\text{m}$ , and then dimpled to  $\sim 30$   $\mu\text{m}$ .

The specimens were ion milled with 3 kV Ar<sup>+</sup> ions and 1 mA current at an incident angle of 12° until perforation was achieved. The microstructure and chemistry of the specimens were investigated by CBED and energy dispersive X-ray spectroscopy (EDS). Magnetic properties of the thin films were measured by using a vibrating sample magnetometer.

Table 1. Deposition conditions of metal/cobalt ferrite composite thin films.

Background pressure	$< 5.0 \times 10^{-6}$ Torr
Sputter gas	10 % O <sub>2</sub> + Ar
Input power	0.8 A × 580 V D. C.
Sputter pressure	$1.0 \times 10^{-3}$ Torr
Deposition rate	200 Å/min
Film composition	28.5 at.% Co-Fe 33.7 at.% Co-Fe 37.8 at.% Co-Fe
Film thickness	0.2 μm
Substrate temperature	Room temperature 200 °C 300 °C 400 °C

### 3. Results and Discussion

Figure 1 shows the variation of magnetic properties of the thin films with the Co content and the substrate temperature. With increasing substrate temperature, the M<sub>s</sub> of the thin films increases and the H<sub>c</sub> of the thin films decreases. This result agrees with that reported by Fujii *et al.* [8] previously. They reported that the oxidation degree of iron oxide thin films was dependent on deposition parameters, e. g., substrate temperature and oxygen partial pressure, and also more-oxidized phases were deposited at low substrate temperatures.

It was also found that the magnetic properties of the thin films depend on the composition. For the hyperstoichiometric composition, Co<sub>37.8</sub>Fe<sub>62.2</sub>, the films with M<sub>s</sub> of ~580 emu/cm<sup>3</sup> and H<sub>c</sub> of 1700 Oe, which might be applicable to the magnetic recording media with high recording density, were prepared in the wide substrate temperature range (200-400 °C). The M<sub>s</sub> value of the films is two to three times higher than that of the conventional cobalt ferrite thin films and the H<sub>c</sub> value is comparable to the conventional metallic thin films [9, 10]. On the other hand, for the near stoichiometric or hypostoichiometric composition, Co<sub>33.7</sub>Fe<sub>66.3</sub> or Co<sub>28.5</sub>Fe<sub>71.5</sub>, the films with magnetic properties needed for the magnetic recording media were prepared in the narrow substrate temperature range (~300 °C).

In addition, it can be seen in Fig. 1 that the magnetic properties of the Co<sub>28.5</sub>Fe<sub>71.5</sub> and Co<sub>33.7</sub>Fe<sub>66.3</sub> thin films change significantly with substrate temperature (200 to 400 °C), while those of the Co<sub>37.8</sub>Fe<sub>62.2</sub> thin films change slightly. In order to understand the dependency of substrate temperature on the magnetic properties, the microstructure of the thin films was investigated.

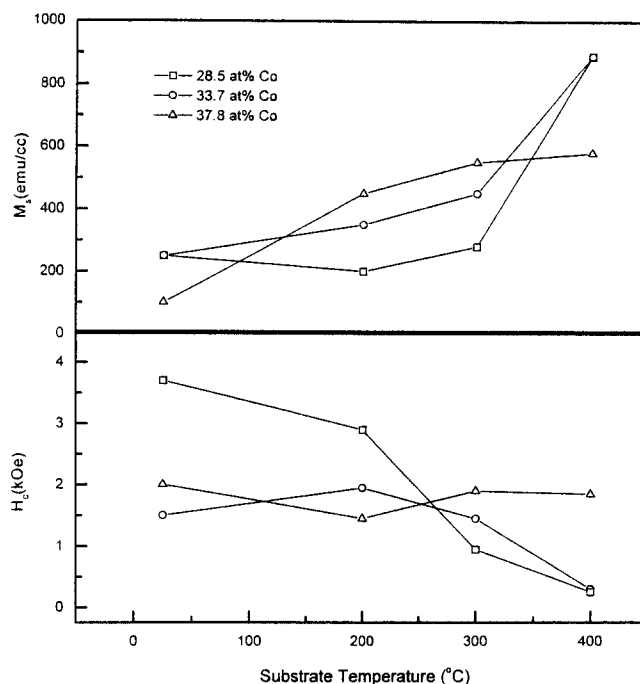


Fig. 1. Variation of magnetic properties of the thin films with the Co content and the substrate temperature.

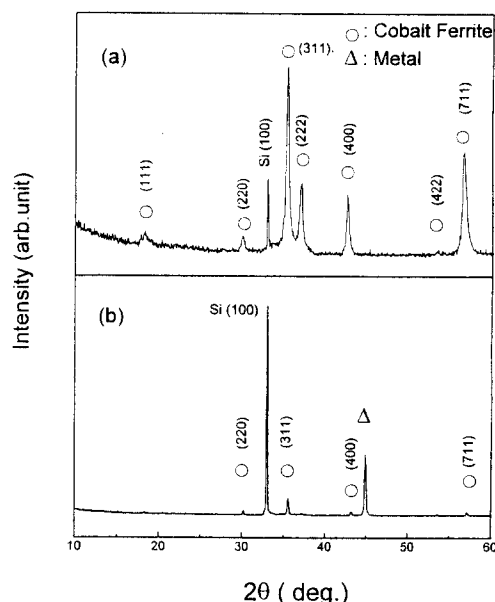


Fig. 2. XRD patterns from the Co<sub>37.8</sub>Fe<sub>62.2</sub> thin films deposited at (a) room temperature and (b) 400 °C substrate temperature.

Figure 2(a) and (b) represent XRD patterns from the  $\text{Co}_{0.78}\text{Fe}_{0.22}$  thin films deposited at room temperature and  $400^\circ\text{C}$ , respectively. For the films deposited at room temperature, only the peak corresponding to cobalt ferrite was detected. On the other hand, for the films deposited at  $400^\circ\text{C}$ , in addition to the peak corresponding to cobalt ferrite, an extra peak was detected. The extra peak may be originated from the precipitation of Co-rich  $\text{Co}_x\text{Fe}_{1-x}$  metal phase in the films. The microstructure and chemistry of the metal and ferrite phases were further investigated by TEM.

Figures 3 (a) and (b) show the cross-sectional bright field images of the  $\text{Co}_{0.78}\text{Fe}_{0.22}$  thin films deposited at 200 and  $400^\circ\text{C}$  substrate temperatures, respectively. It can be seen in Fig. 3

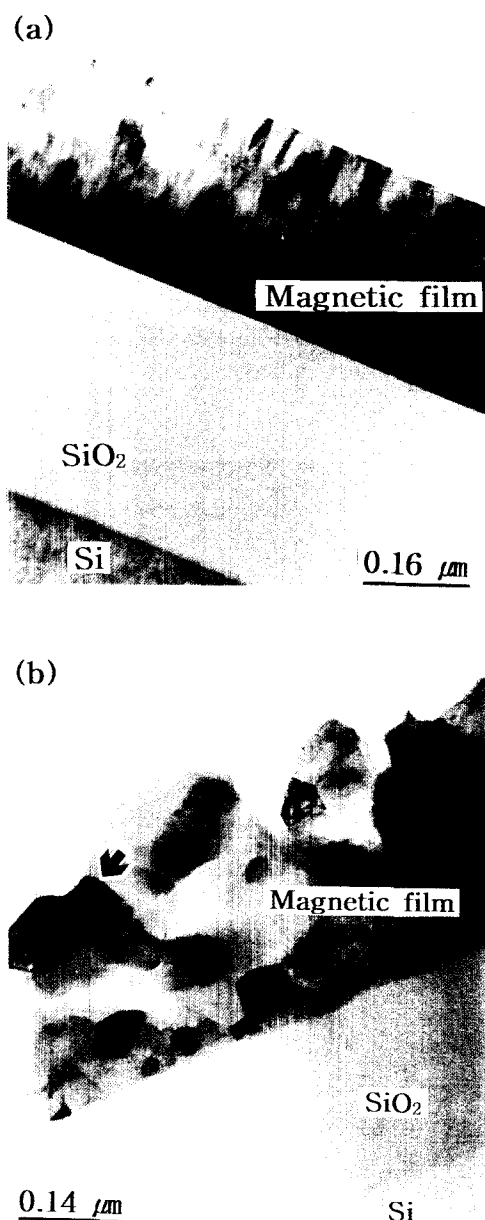


Fig. 3. Cross-sectional bright field images of the  $\text{Co}_{0.78}\text{Fe}_{0.22}$  thin films deposited at (a) 200 and (b)  $400^\circ\text{C}$  substrate temperatures.

that with increasing the substrate temperature the morphology of the thin films was changed from the columnar to granular structure. Especially, at high substrate temperatures ( $>300^\circ\text{C}$ ), Co-rich  $\text{Co}_x\text{Fe}_{1-x}$  alloys were precipitated from the cobalt ferrite. In Fig. 3(b), the Co-rich phase is indicated by an arrow. No chemical reaction was found at the interface between the films and substrates.

Figure 4(a) shows the plan-view bright field image of the  $\text{Co}_{0.78}\text{Fe}_{0.22}$  thin film deposited at  $400^\circ\text{C}$  substrate temperature. The chemistry of cobalt ferrite and Co-rich  $\text{Co}_x\text{Fe}_{1-x}$  metal phases was examined by EDS. Figure 4(b) shows the EDS spectrum obtained from the metal precipitate (marked as an arrow in Fig. 4(a)). In Fig. 4(a), all the grains except the grain indicated by the arrow are cobalt ferrite. The precipitate has a chemical composition of 62 at. % Co and 38 at. % Fe. To identify the microstructure of the precipitate, CBED pattern from the precipitate was obtained first, as shown in Fig. 4(c), and then the primitive cell volume of the precipitate with the three possible crystal structures, i.e., BCC, HCP, and FCC structures, was calculated, as shown in Table 2. Table 2 lists the crystallographic data and theoretical primitive cell volume of the precipitate with the three possible crystal structures.

Table 2. Crystallographic data and theoretical primitive cell volume of the metal precipitate with the three possible crystal structures, i.e., BCC, HCP, and FCC structures.

	BCC	HCP	FCC
Space group	Im3m	P6 <sub>3</sub> /mmm	Fm3m
Lattice parameter (Å)	$a_0 = 2.89$	$a_0 = 2.51$ $c_0 = 4.07$	$a_0 = 3.55$
Unit cell volume (Å <sup>3</sup> )	24.14	22.21	44.74
Primitive cell volume (Å <sup>3</sup> )	12.07	22.21	11.18

The primitive cell volume ( $\Omega$ ) of the precipitate metal phase can be calculated from the CBED pattern shown in Fig. 4(c) using the following equation [7]:

$$\Omega = \frac{2 \cdot L^4 \cdot \lambda^3}{D_1 \cdot D_2 \cdot \sin \alpha \cdot R^2} \quad (1)$$

where  $L$  is the camera length,  $\lambda$  is the wavelength of the electron beam,  $D_1$  and  $D_2$  are the distances from the transmitted to reflected spots,  $\alpha$  is the angle between the two chosen spots, and  $R$  is the radius of the first order Laue zone (FOLZ) ring. The input data for the calculation of the primitive cell volume of the precipitate are given in Table 3. The calculated primitive cell volume of the precipitate is  $11.98 \text{ \AA}^3$ . This primitive cell volume is well matched with the theoretical volume of  $\text{Co}_x\text{Fe}_{1-x}$  ( $x \approx 0.62$ ) with a BCC or FCC structure (Table 2). However, identifying the crystal structure of the metal precipitate is not simple since the primitive cell volume of the  $\text{Co}_x\text{Fe}_{1-x}$  ( $x \approx 0.62$ ) with a BCC structure is closely similar to that of the  $\text{Co}_x\text{Fe}_{1-x}$  ( $x \approx 0.62$ ) with an FCC structure.

Table 3. Summary of Input data for the calculation of the primitive cell volume of the metal phase.

Camera length (L) (mm)	300
Wavelength of electron beam ( $\lambda$ ) (Å)	0.0251
Radius of FOLZ ring (R) (mm)	31.0
Distance of ZOLZ disks ( $D_1$ and $D_2$ ) (mm)	$D_1 = 3.65, D_2 = 6.35$
Angle between disks (degree)	74

To determine the crystal structure of the precipitate, zone axis orientation and corresponding Laue zone spacing at a given zone axis were considered. It was found that BCC structure is suitable for the precipitate. The zone axis of the chosen BCC structure for the metal precipitate was determined by zero order Laue zone (ZOLZ) pattern. The  $[\bar{1}13]$  zone axis is suggested for the CBED pattern shown in Fig. 4(c). For this zone axis, theoretical Laue zone spacing was calculated and then compared with measured value. The Laue zone spacing (H) can be calculated using the following equation [7]:

$$H = \frac{R^2}{2 \cdot \lambda \cdot L^2} \quad (2)$$

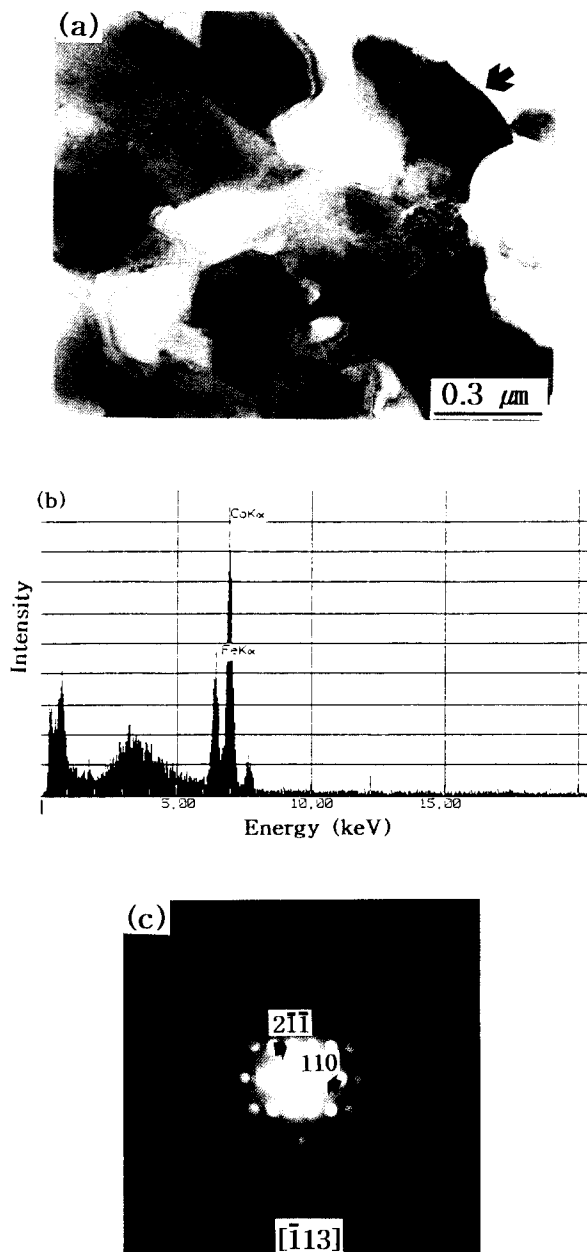


Fig. 4. (a) Plan-view bright field image of the  $Co_{37.8}Fe_{62.2}$  thin film deposited at 400 °C substrate temperature. (b) EDS spectrum and (c) CBED pattern obtained from the metal precipitate indicated by an arrow in (a).

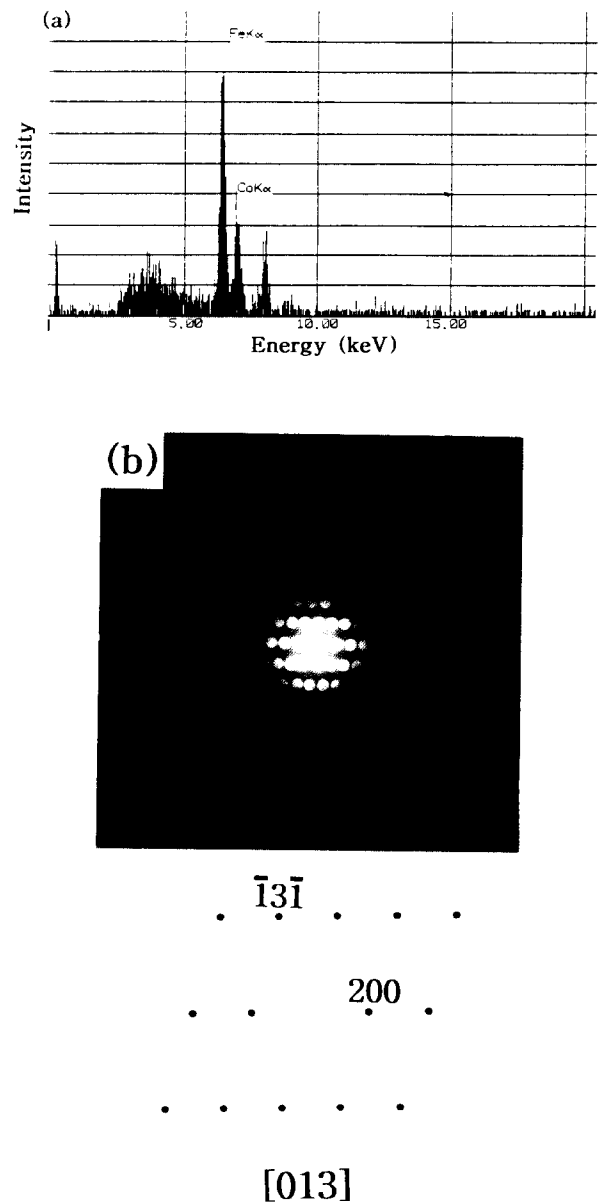


Fig. 5. (a) EDS spectrum and (b) CBED pattern obtained from the cobalt ferrite phase.

The Laue zone spacing calculated from Fig. 4(c) and Eq. (2) for the precipitate is  $0.213 \text{ \AA}^{-1}$ . This value is well matched with the theoretical value ( $0.209 \text{ \AA}^{-1}$ ). Thus, the metal precipitate was identified as  $\text{Co}_x\text{Fe}_{1-x}$  ( $x \approx 0.62$ ) with a BCC structure ( $a_0 = 2.89 \text{ \AA}$ ) and a space group of  $\text{Im}3m$ .

Figures 5(a) and (b) show the EDS spectrum and CBED pattern from the cobalt ferrite phase, respectively. The microstructure of the ferrite phase was identified using the above method. The primitive cell volume calculated from Fig. 5(b) and Eq. (1) for the cobalt ferrite is  $148.1 \text{ \AA}^3$  and the theoretical volume of the cobalt ferrite having a cubic structure ( $a_0 = 8.39 \text{ \AA}$ ) and a space group of  $\text{Fd}3m$  is  $147.6 \text{ \AA}^3$ . ZOLZ pattern was used to determine the zone axis of the chosen cubic structure for the ferrite phase. The zone axis of the CBED pattern shown in Fig. 5(b) was determined as  $[013]$ . The calculated and theoretical Laue zone spacings of the cobalt ferrite are  $0.077$  and  $0.075 \text{ \AA}^{-1}$ , respectively, indicating good agreement between the calculated and theoretical Laue zone spacings. Thus, the ferrite was determined as  $\text{CoFe}_2\text{O}_4$  with a cubic structure ( $a_0 = 8.39 \text{ \AA}$ ) and a space group of  $\text{Fd}3m$ .

Figures 6(a)-(c) show XPS spectra of the  $\text{Co}_{37.8}\text{Fe}_{62.2}$  thin films deposited at room temperature,  $300 \text{ }^\circ\text{C}$ , and  $400 \text{ }^\circ\text{C}$  substrate temperatures, respectively. With increasing substrate temperature, the shape of Co spectra changes significantly, while that of Fe spectra changes slightly. Considering that the  $3\text{P}_{3/2}$  binding energies of Co metal and  $\text{Co}^{2+}$  ion are  $777.9$  and  $780.0 \text{ eV}$  [11], respectively, the shape change of Co spectra indicates

that the Co-rich  $\text{Co}_x\text{Fe}_{1-x}$  metal phase in the thin films increases with increasing substrate temperature. This result agrees with the previous XRD and TEM results.

#### 4. Conclusions

The metal/cobalt ferrite composite thin films with the  $M_s$  of  $\sim 580 \text{ emu/cm}^3$  and the  $H_c$  of  $1700 \text{ Oe}$  were prepared by controlling the sputtering conditions, such as oxygen concentration in sputtering gas, substrate temperature, and composition of the thin films, under a deposition rate of  $200 \text{ \AA/min}$ . With increasing the substrate temperature, the  $M_s$  of the thin films was increased and also the morphology of the thin films was changed from the columnar to granular structure. The thin films deposited at high substrate temperatures ( $> 300 \text{ }^\circ\text{C}$ ) were composed of the  $\text{CoFe}_2\text{O}_4$  phase with a cubic structure ( $a_0 = 2.89 \text{ \AA}$ ) and a space group of  $\text{Fd}3m$  and the  $\text{Co}_x\text{Fe}_{1-x}$  ( $x \approx 0.62$ ) phase with a BCC structure ( $a_0 = 8.39 \text{ \AA}$ ) and a space group of  $\text{Im}3m$ . The  $\text{Co}_x\text{Fe}_{1-x}$  ( $x \approx 0.62$ ) phase could contribute to an increase in the  $M_s$ . For the higher cobalt content than the stoichiometric composition,  $\text{Co}_{37.8}\text{Fe}_{62.2}$ , the thin films with high  $M_s$  and  $H_c$  were obtained in the wide substrate temperature range ( $200\text{-}400 \text{ }^\circ\text{C}$ ). On the other hand, for the near stoichiometric or hypostoichiometric composition,  $\text{Co}_{33.7}\text{Fe}_{66.3}$  or  $\text{Co}_{28.5}\text{Fe}_{71.5}$ , the films with magnetic properties needed for the magnetic recording media were prepared in the narrow substrate temperature range ( $\sim 300 \text{ }^\circ\text{C}$ ).

#### References

- [1] A. N. Okuno, S. Hashimoto, and K. Inomata, *J. Appl. Phys.*, **71**, 5926 (1992).
- [2] J. W. D. Martens, *J. Appl. Phys.*, **59**, 3820 (1986).
- [3] J. C. Slonczewski, *Phys. Rev.*, **110**, 1341 (1958).
- [4] Y. Le Page and D. Downham, *J. Electron Microsc. Tech.*, **18**, 437 (1991).
- [5] C. Narayan, *J. Electron Microsc. Tech.*, **3**, 151 (1986).
- [6] D. B. Williams, *Practical Analytical Electron Microscopy in Materials Science*, Philips Electron Instruments, New Jersey (1988) pp. 117-146.
- [7] G. H. Kim, H. S. Kim, and D. W. Kum, *Microsc. Res. Tech.*, **33**, 510 (1996).
- [8] T. Fujii, M. Takano, Y. Bando, and Y. Isozumi, *J. Appl. Phys.*, **66**, 3168 (1989).
- [9] J. W. Martens, *J. Appl. Phys.*, **59**, 3820 (1986).
- [10] J. C. Milaan and R. D. Fisher, *IEEE Trans. Magn.*, **23**, 122 (1987).
- [11] G. E. Muilenberg, *Handbook of x-ray photoelectron spectroscopy*, Perkin-Elmer Co., Eden Prairie (1979) pp. 76-79.

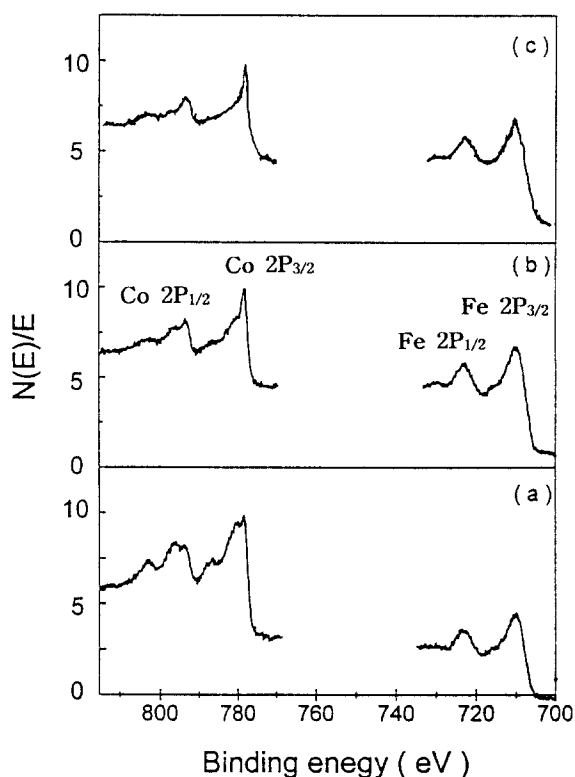


Fig. 6. XPS spectra of the  $\text{Co}_{37.8}\text{Fe}_{62.2}$  thin films deposited at (a) room temperature, (b)  $300 \text{ }^\circ\text{C}$ , and (c)  $400 \text{ }^\circ\text{C}$  substrate temperatures.